Silver carbonate nanoparticles stabilised over alumina nanoneedles exhibiting potent antibacterial properties†

Joanna J. Buckley,[a] Pratibha L. Gai,[abc] Adam F. Lee,*[a] Luca Olivi[d] and Karen Wilson*[a]

Received (in Cambridge, UK) 29th May 2008, Accepted 27th June 2008
First published as an Advance Article on the web 17th July 2008
DOI: 10.1039/b809086f

A simple method of preparing Ag_2CO_3 nanoparticles utilising high area γ-alumina nanoneedles has been developed; these are promising antimicrobial agents against diverse bacterial strains.

Around 80% of hospital acquired infections are associated with bacterial adhesion at surfaces of medical devices and biomaterials, with an annual estimated cost to hospitals and the workforce of $30 billion in the US alone.[1]

Antimicrobial agents, often applied in coatings, are important for imparting sterility and the ability to prevent infection. Silver is the most widely used such agent for wound care, due to its ability to kill a broad spectrum of infectious bacteria. Its use against pathogens is well established,[2] dating back to ancient Greece where silver coins were placed in water to inhibit bacterial growth.[3] Since silver's first clinical application as a dilute nitrate solution to treat eye infections and infant blindness,[4] both the utility and presentation format have diversified. Silver sulfadiazine is widely employed to treat infections,[5] while silver coated catheters help to reduce biofilm formation,[6,7] and new silver dressings[8] that can obviate and complement grafting are now commercially available for burns.[9] It is widely held that the release of free silver ions is crucial to the performance of all antibacterial silver formats.

Nanoparticulate silver has shown much recent promise as an antibacterial and antifungal agent,[10] with both size-[11] and shape[12]-dependent microbiological activity reported for large metallic clusters. However such free nanoparticles are an unsuitable presentation format for medical devices such as wound dressings, where confined, topical application and prolonged silver release are needed.[13] There are fewer microbiological studies on supported Ag nanoparticles, and these generally utilise polymeric frameworks, which show poor pH/solvent and thermal tolerances[14] or poor bacterial inhibition.[15] Small (~7 nm) silver nanoparticles, synthesised on silica nanospheres, have shown promise against *S. enterica* serovar Typhimurium,[16] while Ag–SiO_2–cotton composites inhibit *E. coli*.[17] However, accurate microactivity tests have not been conducted for such inorganic supports, and the nanoparticles themselves remain poorly characterised. We recently demonstrated the use of a transitional mesoporous alumina phase to stabilise dispersed Pd clusters in a high oxidation state.[18] In light of this discovery, we have explored whether the same hydrophilic alumina support could generate ionic silver clusters, and therefore promote bacteriostasis, while minimising silver loadings and potential toxicity issues.[19] Here we report the synthesis of supported nanoparticulate silver carbonate, which exhibits remarkable bactericidal activity in simulated wound environments against both Gram-positive and -negative strains.

A mesoporous alumina support was prepared by a modified surfactant-templated route through hydrolysis of aluminium *sec*-butoxide and subsequent aging with lauric acid prior to calcination (see ESI†).[20] Porosimetry and X-ray diffraction confirmed that the initial alumina support possessed well-defined, hexagonal pores around 3.5 nm diameter, with a BET surface area of 350 $m^2\ g^{-1}$. Silver doping was achieved by incipient wetness impregnation of the pre-synthesised alumina with $AgNO_3$ and subsequent calcination, and air-storage. The silver loading was varied between 0.15 and 6.21 wt%.

The morphology and structure of the ultra-dilute Ag-doped alumina support were first imaged by double aberration-corrected (scanning) transmission electron microscopy (Fig. 1). This evidences a striking transformation in the support, from a thick-walled, mesoporous transitional alumina framework, to interconnected γ-Al_2O_3 needles (platelets) upon silver doping. Similar nanoneedles have been observed upon base etching of porous alumina, or annealing boehmite,[21] and we are currently exploring the mechanism of this directed recrystallisation. Standard dark-field imaging also highlights small Ag-rich nanoparticles that decorate the γ-alumina needles. These nanoparticles lie between 3–5 nm, and exhibit lattice parameters characteristic of β-Ag_2CO_3 and single-crystallinity. The genesis of such nanoneedles in the presence of Ag-rich nanoparticles may also open new routes to preparing alumina nanostructures.

The global chemical environment of dispersed silver was also examined by bulk and surface sensitive X-ray methods. Linear combination fitting of the Ag K-edge X-ray absorption near-edge structure (XANES) spectra for both ultra-dilute and 6.21 wt% Ag/meso-Al_2O_3 materials revealed an excellent fit to Ag_2CO_3 (Fig. 2), in accordance with the preceding microscopy. Auger parameter analysis of the corresponding Ag 3d

[a] *Department of Chemistry, University of York, York, UK YO10 5DD. E-mail: afl2@york.ac.uk; Fax: +44 1904 434470 Tel: +44 1904 432516*
[b] *York JEOL Nanocentre, Helix House, University of York, York, UK*
[c] *Department of Physics, University of York, York, UK YO10 5DD*
[d] *Sincrotrone Trieste, 34012 Basovizza, Trieste, Italy*
† Electronic supplementary information (ESI) available: Full materials synthesis, characterisation and antibacterial protocols. See DOI: 10.1039/b809086f

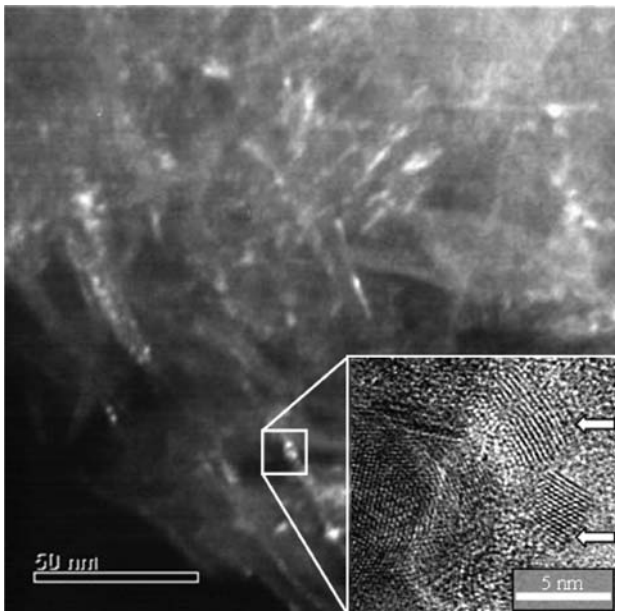

Fig. 1 Morphology and structure by TEM: dark-field image of 0.15 wt% Ag/meso-Al_2O_3 showing nanoparticulate silver as bright spots. Inset shows ACTEM bright-field image of β-Ag_2CO_3 nanoparticles.

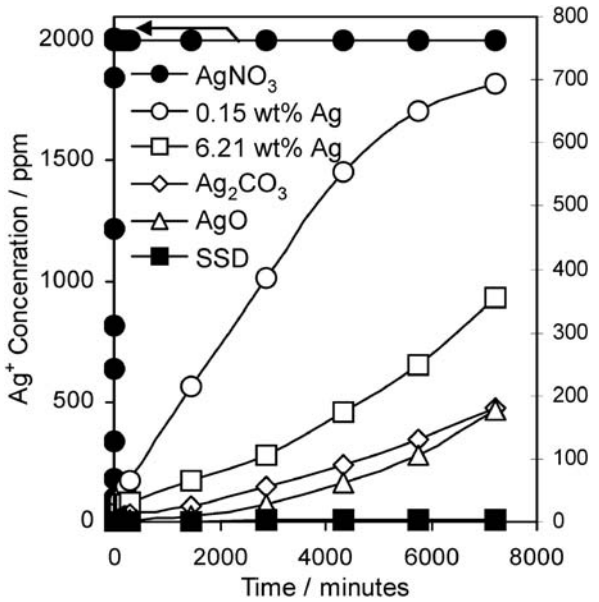

Fig. 3 Silver dissolution rates from Ag/meso-Al_2O_3 and standards in aqueous buffered solution; each sample contained the same mass of silver.

and $M_{4,5}NN$ transitions by X-ray photoelectron spectroscopy (XPS) confirms that the surfaces of these nanoparticles are also carbonate terminated, with a surface Ag : CO_3 atomic ratio of 1.7 : 1.†

It is generally accepted that the inhibitory action of silver upon microorganisms is linked to the impact of aqueous Ag^+ ions upon essential cellular proteins[22] and DNA replication.[23] The release rates of ionic silver from the ultra-dilute and high loading Ag/meso-Al_2O_3 samples were therefore compared with those from bulk silver compounds (Fig. 3). As expected, silver nitrate dissolved essentially instantly on contact with an aqueous solution. However an exciting observation was that Ag^+ dissolution rates from the Ag_2CO_3 nanoparticles far outstrip those of bulk silver oxides or carbonate. The ultra-dilute Ag/meso-Al_2O_3 releases silver ions much faster than the commercial (and poorly soluble) silver sulfadiazine complex (SSD), and significantly faster than the higher loading 6.21 wt% material which comprised larger silver carbonate nanocrystals (~30 nm). It is important to note that silver release from SSD is sensitive to wound pH and the presence of sodium salts and proteins in tissue fluid.[9] Synergic interactions between Ag^+ ions slowly released from the silver sulfadiazine polymer matrix,[24] and sulfadiazine ligands themselves, may compensate for the low level of dissolved silver (which in turn limits depletion of body electrolytes) and contribute to the observed efficacy of SSD.[25]

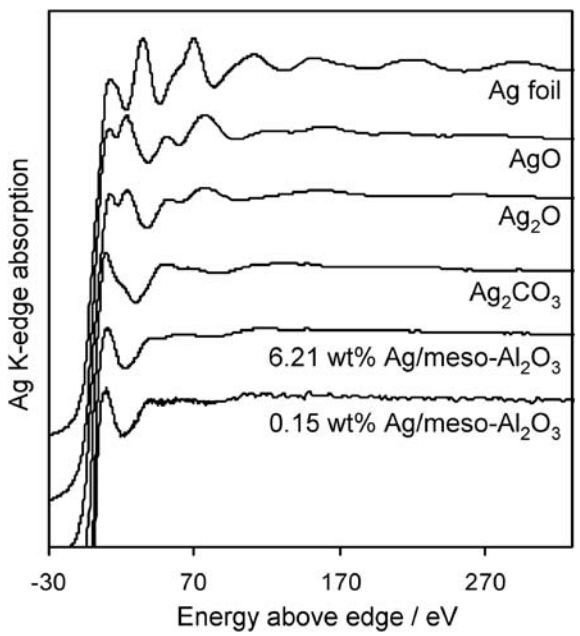

Fig. 2 Normalised Ag K-edge XANES for Ag/meso-Al_2O_3 materials and comparative Ag standards.

The antimicrobial activity of the Ag/meso-Al_2O_3 sample was assessed by both zone plate inhibition and the logarithmic reduction method against *Staphylococcus aureus* NCTC 10788 and *Pseudomonas aeruginosa* NCIMB 8626, respective Gram-positive and -negative bacteria found on the skin and in chronic wounds. Zone assay plates were seeded with test organisms to which each silver sample was added. Plates were subsequently incubated, and any resultant clear zone surrounding the sample (where bacterial growth was inhibited) compared to bulk silver standards. The normalised zone of inhibition of the supported Ag_2CO_3 nanoparticles far exceeds that of bulk AgO, Ag_2CO_3 and Ag_2O per unit mass of silver.† Indeed the antibacterial performance of alumina-supported materials exhibits a striking increase with decreasing silver content and corresponding Ag_2CO_3 nanoparticle size. Simple geometric considerations suggest that zone size is directly proportional to the carbonate surface area.† Ag/meso-Al_2O_3 samples were effective against both Gram-positive and -negative bacteria, performing slightly better against *S. aureus*.

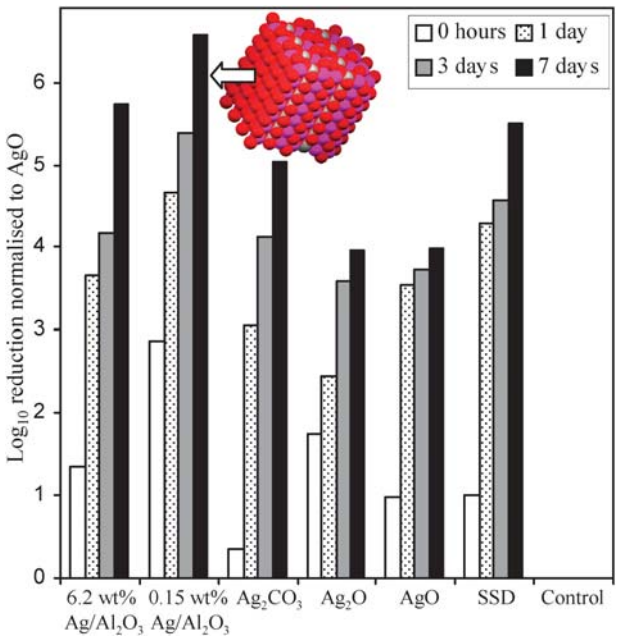

Fig. 4 Bacterial kill tests for Gram-positive *S. aureus* NCTC 10788. For ease of comparison data are normalised to the mass of silver in AgO.

These semi-quantitative measurements give a good indication of antimicrobial activity but do not provide information on bacterial kill rates which are far more important in wound management. A full quantitative kill test was subsequently performed over a 7 day period with Gram-positive *S. aureus* NCTC 10788. This organism was chosen as it is resistant to silver and its thick peptidoglycan cell wall renders it particularly hard to kill. Ag/meso-Al_2O_3 was inoculated with *S. aureus* and incubated for a week. Antimicrobial activity is assayed from the decrease in viable bacteria after specific times. The $\log_{10}$ reduction is obtained by subtracting the log of the microorganism count at each time point from the equivalent count in the fresh inoculum: one log reduction unit therefore represents a 90% kill efficiency. These kill tests confirm the remarkable activity of our supported Ag_2CO_3 nanoparticles, which are able to kill *S. aureus* for over 7 days, outperforming their bulk counterparts by over 2 log units, equating to >100-fold enhancement per mass of silver. The ultra-dispersed 5 nm Ag_2CO_3 nanocrystals even exceed SSD, which is widely used as a topical dilute solution for severe burns and ulcers. The anomalous behaviour of SSD, which Fig. 4 reveals is an effective antibacterial agent despite its poor silver release rate, may reflect the action of the dissociated sulfadiazene product (itself a bacteriostatic antibiotic[25]), coupled with greater silver solubility in the presence of the nutrient broth used in the kill tests compared with the electrochemical study in Fig. 3. This is not the case for the remaining silver standards or supported carbonate nanoparticles, wherein dissolved silver ions represent the only active component. It is also interesting to note that unsupported Ag_2CO_3 is a more potent bactericide than either oxide standard; the latter have been postulated as the active silver species in wound dressings.[26] We believe the alumina nanoneedle support is crucial for stabilising highly dispersed Ag_2CO_3 and are currently investigating the recrystallisation mechanism.

The link between silver carbonate nanoparticle size and loading also offers a simple means to tune the release rate of ionic silver and thus device application. Unlike many other silver presentations, these nanoparticles are air- and photostable. They are also cheap to produce on the kiloscale, nontoxic or allergenic and do not stain the skin, and may have potential within the expanding antimicrobials market.

We thank the University of York, JEOL, Yorkshire Forward and the ERDF for support of the York JEOL Nanocentre. J.J.B. thanks Smith & Nephew for funding, and T. Deakin (York Physics) and P. Gunning (Smith & Nephew) for assistance with SEM.

Notes and references

1 I. M. Gould, *Int. J. Antimicrob. Agents*, 2006, **28**, 379; http://www.hospitalinfection.org/costofinfection.shtml (February 2008).
2 J. Gibbard, *J. Am. Public Health*, 1937, **27**, 122.
3 W. R. Hill and D. M. Pillsbury, *Argyria—The Pharmacology of Silver*, Williams and Wilkins, Baltimore, 1939.
4 F. W. Newell, *Am. J. Ophthalmol.*, 1980, **90**, 874.
5 C. Fox, *Int. Surg.*, 1975, **60**, 275.
6 P. Thibon, X. Le Coutour, R. Leroyer and J. Fabry, *J. Hosp. Infect.*, 2000, **45**, 117.
7 M. E. Rupp, T. Fitzgerald, N. Marion, V. Helget, S. Puumala, J. R. Anderson and P. D. Fey, *Am. J. Infect. Cont.*, 2004, **32**, 445.
8 M. Ip, S. Lai Lui, V. K. M. Poon, I. Lung and A. Burd, *J. Med. Microbiol.*, 2006, **55**, 59.
9 H. J. Klasen, *Burns*, 2000, **26**, 131; B. S. Atiyeh, M. Costagliola, S. N. Hayek and S. A. Dibo, *Burns*, 2007, **33**, 139.
10 I. Sondi and B. Salopek-Sondi, *J. Colloid Interface Sci.*, 2004, **275**, 177.
11 J. R. Morones, J. L. Elechiguerra, A. Camacho, K. Holt, J. B. Kouri, J. T. Ramirez and M. J. Yacaman, *Nanotechnology*, 2005, **16**, 2346.
12 S. Pal, Y. K. Tak and J. M. Song, *Appl. Environ. Microbiol.*, 2007, 1712.
13 R. Kumar and H. Münstedt, *Biomaterials*, 2005, **26**, 2081.
14 W.-F. Lee and K.-T. Tsao, *J. Appl. Polym. Sci.*, 2006, **100**, 3653.
15 D. P. Dowling, K. Donnelly, M. L. McConnell, R. Eloy and M. N. Arnaud, *Thin Solid Films*, 2001, **398**, 602.
16 S.-D. Oha, S. Lee, S.-H. Choi, I. S. Lee, Y.-M. Lee, J. H. Chun and H. J. Park, *Colloids Surf., A*, 2006, **275**, 228.
17 S. Tarimala, N. Kothari, N. Abidi, E. Hequet, J. Fralick and L. L. Dai, *J. Appl. Polym. Sci.*, 2006, **101**, 2938.
18 S. F. J. Hackett, R. M. Brydson, M. H. Gass, I. Harvey, A. D. Newman, K. Wilson and A. F. Lee, *Angew. Chem., Int. Ed.*, 2007, **46**, 8593.
19 A. B. G. Lansdown and A. Williams, *J. Wound Care*, 2004, **13**, 131.
20 F. Vaudry, S. Khodabandeh and M. E. Davis, *Chem. Mater.*, 1996, **8**, 1451.
21 B. Tang, J. Ge, L. Zhuo, G. Wang, J. Niu, Z. Shi and Y. Dong, *Eur. J. Inorg. Chem.*, 2005, 4366.
22 M. Yamanaka, K. Hara and J. Kudo, *Appl. Environ. Microbiol.*, 2005, **71**, 7589.
23 Q. L. Feng, J. Wu, G. Q. Chen, F. Z. Cui, T. N. Kim and J. O. Kim, *J. Biomed. Mater. Res.*, 2000, **52**, 662.
24 N. C. Baenziger and A. W. Struss, *Inorg. Chem.*, 1976, **15**, 1807.
25 C. L. Fox, Jr and S. M. Modak, *Antimicrob. Agents Chemother.*, 1974, **5**, 582.
26 B. Halford, *Chem. Eng. News*, 2006, **84**, 35.